Carpathian Journal of Earth and Environmental Sciences, February 2015, Vol. 10, No. 1, p. 121 - 132

PETROLOGY AND GEOCHEMISTRY OF DOLERITIC DYKE OF LIKOK (CAMEROON, CENTRAL AFRICA)

Oumarou Faarouk NKOUANDOU[1*], Aminatou MEFIRE FAGNY[2], Gabriel Ovidiu IANCU[3] & Jacques-Marie BARDINTZEFF[4,5]

*[1]Faculty of Science, University of Ngaoundéré, P.o. Box. 454 Ngaoundéré-Cameroon, *Corresponding author address: ofaarouk@yahoo.fr*

[2]Faculty of Science, University of Ngaoundéré, P.o. Box. 454 Ngaoundéré-Cameroon, afagny2002@yahoo.fr

[3]Faculty of Geography and Geology, University of Alexandru Ioan Cuza, Iaşi, Romania, 700505-RO, Iaşi, Bulevardul Carol I nr. 20A (ogiancu@yahoo.com)

[4,5]University of Paris-Sud, Laboratoire IDES, UMR 8148, Bât. 504, F−91405 Orsay, France: email address: jacques-marie.bardintzeff@u-psud.fr Tel. (33) (1) 69 15 67 44

Abstract: Dolerites dyke swarm trending N70, N135 and E-W transect the Pan-African granitic rocks of Likok area (Adamawa plateau-Cameroon) in Central Africa. Petrography, mineral chemistry and geochemical compositions of those rocks have been attempted for the first time. Dolerites exhibit a coarse-grained porphyroid and sub-ophitic doleritic texture. Microprobe analyses show that they are composed of diopside ($Wo_{49.27}En_{41.92}Fs_{8.81}$), subcalcic augite ($Wo_{25.41–41.93}$ $En_{42.34–46.61}$ $Fs_{11.37–31.80}$) and pigeonite clinopyroxene ($Wo_{18.64}$ $En_{46.12}$ $Fs_{35.24}$). Plagioclases are labrador ($Ab_{34.74–46.25}$ $An_{51.15–63.40}$), andesine ($Ab_{55.14–64.54}$ $An_{35.12–44.96}$), oligoclase ($Ab_{76.97–85.96}$ $An_{1.27–22.61}$) and albite ($Ab_{92.42–93.76}$ $An_{5.64–6.38}$). Alkali feldspar is dominantly orthoclase ($Or_{72.97–97.97}$ $Ab_{1.83–25.73}$). Biotite, titanomagnetite, ilmenite, apatite and titanite are accessory phases. XRF whole-rock chemical analysis highlight two distinct dolerites of group I (Mg: 53.0%) and group II (Mg: 62.0−65.0%) compositions. All dolerites belong to low-Ti quartz-normative continental tholeiites, generated from the enriched sub-continental lithospheric mantle. The similar characteristics are displayed by the neighboring dyke swarm from Biden (Cameroon) and Obudu (Nigeria), arguing for a common early stage setting of Pan-African break-up, initiated in Late Jurassic-Early Cretaceous time.

Keywords: petrology, geochemistry, dolerite, geodynamic, Likok, Cameroun, Central Africa.

1. INTRODUCTION

Dolerite dyke swarms mostly represent the late magmatic episode occurring in the extensional and tectonic setting (Essany & El−Metwally, 1999; Worthing, 2005), thus inferring the key elements to understand the geodynamic processes (Reeves, 2000; Srivastava, 2011). Magma mixing, fluid circulation and crustal contamination generally affect the fractional crystallization process behind their evolution (Seymour & Kumarapeli, 1995; Marzoli et al., 2006). Numerous dolerite dykes crosscut the Pan-African granitoid basement rocks of the Cameroon Volcanic Line (Béa et al., 1990; Ngounouno et al., 2001), Adamawa plateau (Vicat et al., 2001) and Neoproterozoic metamorphic gneiss of northern Cameroon Congo craton (Vicat et al., 1997), in Central Africa. Few have been studied in detail and their petrography, geochemistry and geochronology have been constrained. The dolerite dyke swarms of Likok in Adamawa plateau have been sampled recently and have never being studied in detail.

This work is focused on the petrography, mineral chemistry and whole-rock analysis of Likok dolerite dyke swarm (Adamawa plateau) to constrain their petrogenesis and hence the tectonic evolutions of the underlying crust.

2. GEOLOGICAL SETTING

The Adamawa plateau and Cameroon Volcanic Line (CVL) basement rocks belong to the Central Africa Pan-African Fold Belt (CAPFB, Fig. 1).

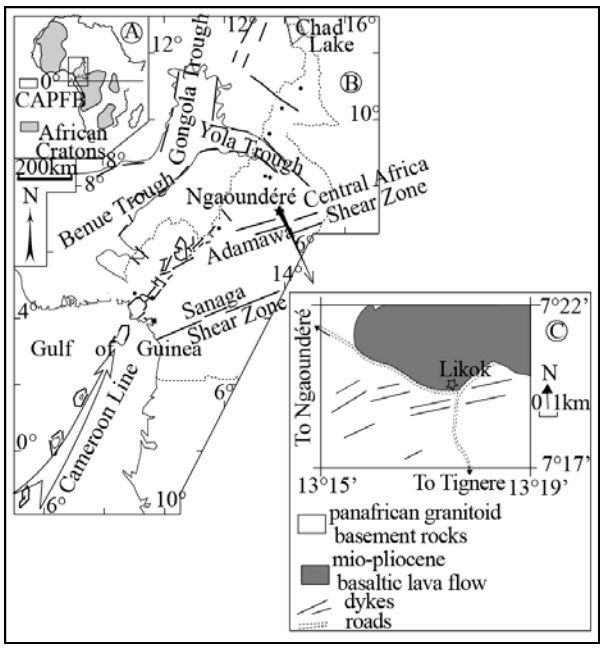

Figure 1. Geological sketch map of Likok (C). Inset (B): the Cameroon Volcanic Line (arrow) and Benue trough after Déruelle et al., (2007). Upper inset (A): relationships between the Cameroon Volcanic Line and African cratons after Kampunzu & Popoff (1991).

This inter-cratonic zone is part of a weakened and remobilized Gondwanian assemblage of Paleozoic and Mesozoic ages (Popoff, 1988). It is composed of granite and migmatite of Pan-African age (550 ± 100 My) or syn- to post-tectonic granitoid of 615 ± 27 My Th−U−Pb age (Ganwa et al., 2008 ; Tchameni et al., 2006). Previous studies have mentioned the occurrence of multitudinous dyke swarm intruding the Cameroon volcanic basement rocks. Two doleritic episodes of back-arc basin and greenstone belt tholeiites type (Paleoproterozoic in age) of typical continental tholeiites, respectively, (Neoproterozoic in age) have been distinguished (Vicat et al., 1997) in this area. They have been interpreted (Vicat et al., 1997) as the result of Eburnean and Pan-African orogenic cycle initiation. In the Adamawa plateau, at Biden, old dolerite dyke of continental tholeiite display negative Nb, Ta and Ti anomalies, attesting their sub-continental mantle origin (Vicat et al., 2001). They have been interpreted as indicating an early stage of continental break-up, which was contemporaneous or predating the Cretaceous tholeiitic magmatism of predominantly asthenospheric origin (Vicat et al., 2001). Tertiary basaltic dyke of continental tholeiitic affinity intrude the metamorphic-granitic basement, coeval with the infilling of Cretaceous Yola in Garoua grabens (Bea et al., 1990). They are related to the Ordovician and Devonian extensional tectonics, responsible for the opening of the small aulacogens at the northern Cameroon (Bea et al., 1990). Dolerite dykes of Likok crosscut the continental Pan-African granitoid rock, 45 km from Ngaoundéré.

3. MATERIALS AND METHODS

20 thin sections have been made on the selected representative samples at the University of Paris-Sud, Orsay. Mineral analyses have been performed with the microprobe CAMECA SX 100 of the Service Camparis, Paris VI. The operating conditions were an accelerating voltage and a beam current as follows: clinopyroxene: 15 kV and 40 nA, 20 s except Ti for clinopyroxene (30 s); plagioclase, K-feldspar, nepheline and nosean: 10 s; titanomagnetite: Si, Ca, Ni: 10 s; Mn: 25 s; Cr; 15 s; Al: 30 s; Ti, Fe, Mg: 40 s. Standards used were a combination of natural and synthetic minerals. Data corrections were made using a PAP method correction of Pouchou & Pichoir (1991). Major element and significant trace element analyses of lavas were determined through energy-dispersive X-ray fluorescence spectroscopy (ED-XRF), using an ED-XRF Epsylon 5 Spectrometer at the Department of Geology, Faculty of Geography and Geology, University of Alexandru Ioan Cuza, of Iasi, Romania, after a previous ground of the samples and their mix with Hoechst wax. The spectrometer calibration was performed by using standards provided by Geological Survey of Japan, CCRMP-CANMET-MMSL, Natural Resources Canada and USGS of United States Geological Survey.

4. RESULTS

4.1. Nomenclature

According to the mineral composition, analysed samples exhibit a tholeiitic affinity with the occurrence of a few percent (< 2 wt%) pigeonite and low Ca-clinopyroxene, expressed as the groundmass components. The Likok whole-rock analyses have been plotted in several geotectonic and rock nomenclatorial diagrams (Fig. 2 and 3).

Accordingly, all rocks belong to the continental tholeiites series as suggest their Th/Ta ratios (2.0—5.0) (Cabanis & Thieblemont, 1988). The occurrence of modal quartz in groundmass (< 3 wt %) of all samples attests their quartz tholeiite affinity. The Nb/Y vs Zr/P_2O_5 (Floyd & Winchester, 1975, Figure not shown) and the Y/Nb ratios (1.1−3.4, Pearce & Cann, 1973) also substantiate these considerations.

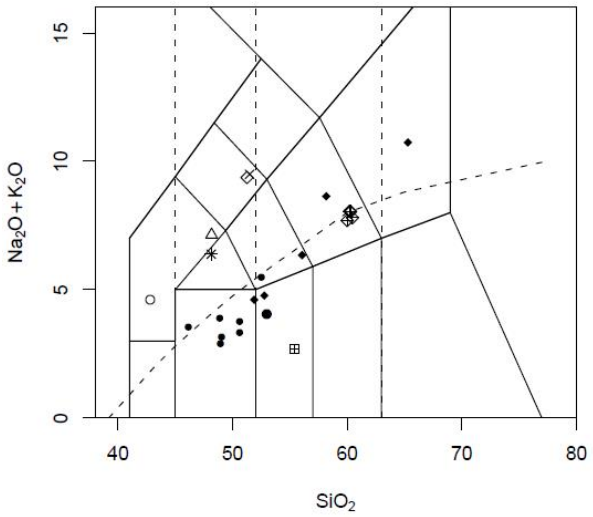

Figure 2. Classification alkalis vs. SiO2 diagram for of Likok (asterisk, open triangle) and Hama Koussou (dashed square and cycle) dolerites (Le Bas et al., 1986)

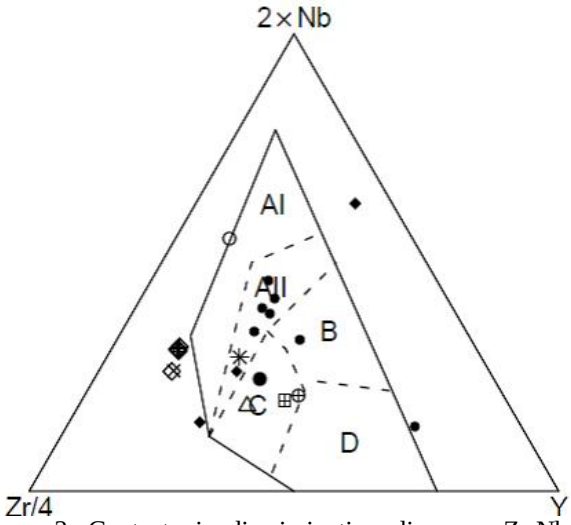

Figure 3. Geotectonic discrimination diagrams Zr-Nb-Y **(**Meschede, 1986**)** for doleritic dyke swarm of Likok (asterisk, open triangle respectively in fields AII and C) and Hama Koussou (dashed square and cycle in field C). The rests are from Vicat et al., (2001).The fields are: A1, within plate basalts, A11, within plate alkali basalts and within plate tholeiites; B, E-type MORB; C, within plate tholeiites and volcanic arc basalts; D, N-type MORB and volcanic arc basalts.

4.2. Field work and petrography

Studied dykes swarms are vertical to subvertical and are 10 to 15 meters, thus belong to giant dyke swarms (Bryan & Ernst, 2008). They are dark grey in color and are frequently crosscutting by the thin (0.5 to 2.0 cm) light apophysis of quartz and feldspar in composition. The main directions are parallel to Pan-African orientation N070E, N160E and E-W suggested by Moreau et al., (1987). Likok samples present coarse-grain porphyroid texture where plagioclase crystals with an elongated tabular habit are sub-ophitic intergrown with the clinopyroxene or partially enclosed in augite phenocrysts. Crystals of biotite have sharp and sometimes frayed ends. Green brownish skeletal crystals of hornblende are present and are destabilised in edges into corona of oxides phenocrysts. Phenocrysts of greenish clinopyroxene always aggregate with those of hornblende (destabilized) and oxides into glomeroporphyric texture, as a consequence of minerals accumulation. In this assemblage, feldspar crystals, mainly plagioclase, show the alteration sign with spots and fuzzy twins. Abundant crystals of alkali feldspar constitute the groundmass. All those crystals present the entire or partial inclusion of oxides microcryst and minute crystals of elongated apatite. Microprobe analyses revealed the presence of trydimite microcrysts and a few percent (< 2 wt%) of titanite in the groundmass. Rare gosh of titanite are suspected. Altered clinopyroxene phenocrysts show the small yellowish beaches with abundant oxides inclusion.

4.3. Mineralogy

Clinopyroxene chemical analyses are presented in table 1 and their compositional variation is illustrated in figure 4. Three types of such phases are distinguished following the classification of Morimoto et al. (1988): diopside type with $Wo_{49.27}\ En_{41.92}\ Fs_{8.81}$, subcalcic-augite type, and clinopyroxene ($Wo_{25.41-41.93}\ En_{42.34-46.61}\ Fs_{11.37-31.80}$) and Ca-poor clinopyroxene belonging to the pigeonite type ($Wo_{18.64}\ En_{46.12}\ Fs_{35.24}$). There is a continuous decrease in Wo contents from diopside to pigeonite and a lateral increase in Fe^{2+} contents from calcic pyroxene to Fe-rich hedenbergite (Fig. 4).

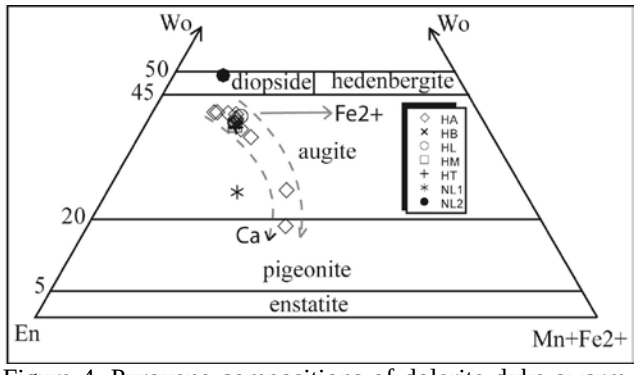

Figure 4. Pyroxene compositions of dolerite dyke swarm of Likok. Black and green dashed arrows illustrate the evolution of pyroxene crystal compositions from Ca-riche to Ca-poor magma during differentiation. Horizontal black arrow indicates the second possibility of $Mg \rightarrow Fe^{2+}$ diminution during pyroxene crystallization.

Table 1. Representative microprobe analyses of clinopyroxene of doleritic dykes of Likok. ph, c: phenocryst core

sample	HA	HB	HA		HM	HA			NL2	NL1
description	Ph, c									
SiO_2 (wt %)	55.03	50.34	58.07	50.45	48.61	49.65	50.26	49.65	52.30	54.23
TiO_2	0.01	0.31	0.00	0.30	0.68	0.54	0.38	0.55	0.04	0.01
Al_2O_3	0.73	3.53	1.20	3.18	5.09	4.17	3.91	3.34	1.06	3.25
Cr_2O_3	0.01	0.00	0.03	0.01	0.00	0.00	0.01	0.01	0.27	0.02
Fe_2O_3	0.00	2.77	0.00	2.80	3.36	2.63	1.73	4.76	3.66	0.00
FeO	17.94	8.87	17.89	8.56	8.60	8.45	10.98	6.80	5.45	12.86
MnO	0.40	0.42	0.40	0.29	0.31	0.27	0.29	0.29	0.39	0.38
MgO	13.40	13.57	13.13	13.32	12.78	13.14	13.20	13.69	13.34	15.96
CaO	12.02	19.49	8.20	20.19	19.32	19.87	18.10	20.45	23.42	12.75
Na_2O	0.09	0.44	0.18	0.46	0.50	0.48	0.53	0.47	0.64	0.36
sum	99.63	99.73	99.10	99.55	99.26	99.21	99.39	100.00	100.56	99.84
Si (a.p.f.u.)	2.111	1.890	2.244	1.898	1.838	1.872	1.897	1.860	1.943	2.021
Ti	0.000	0.009	0.000	0.008	0.019	0.015	0.011	0.016	0.001	0.000
Al	0.033	0.156	0.055	0.141	0.227	0.185	0.174	0.147	0.047	0.143
Cr	0.000	0.000	0.001	0.000	0.000	0.000	0.000	0.000	0.008	0.001
Fe+++	0.000	0.078	0.000	0.079	0.096	0.075	0.049	0.134	0.102	0.000
Fe++	0.575	0.278	0.578	0.269	0.272	0.266	0.347	0.213	0.169	0.401
Mn	0.013	0.013	0.013	0.009	0.010	0.009	0.009	0.009	0.012	0.012
Mg	0.766	0.759	0.756	0.747	0.720	0.739	0.743	0.765	0.739	0.887
Ca	0.494	0.784	0.340	0.814	0.782	0.803	0.732	0.821	0.932	0.509
Na	0.007	0.032	0.013	0.034	0.036	0.035	0.039	0.034	0.046	0.026
Wo (wt %)	25.86	39.48	18.64	41.45	39.17	40.65	36.71	41.93	49.27	25.41
En	42.34	44.79	46.12	43.53	44.83	44.05	43.26	46.61	41.92	51.38
Fs	31.80	15.74	35.24	15.03	16.00	15.29	20.03	11.47	8.80	23.22

All pyroxenes have low TiO_2 contents (< 0.7 wt%). Al_2O_3 contents are low (< 1 wt%) in Ca-poor clinopyroxene and relatively high Ca-rich clinopyroxene (2−5 wt%). Al^{VI} vs Al^{IV} (Figure not shown) shows that Ca-poor clinopyroxene crystallized at high pressure and Ca-rich clinopyroxene crystallized at low pressure. This may attest that Ca-poor clinopyroxene crystallised before Ca-rich clinopyroxene. In this study, the minor amounts of Ca-rich and Ca-poor clinopyroxene render this order difficult to confirm. Thus, it remains complex to know precisely which phase crystallised before. Pigeonite crystals are characterised by their high Mg (Mg = Mg/(Mg+Fe)) contents (0.6−0.7). The Mg-Fe (Mg-Fe exchange between coexisting pigeonite-augite) partitioning coefficient K_D (= (Mg pigeonite/(1-Mg))*((1-Mg)augite/Mg augite) are calculated assuming that all iron are ferrous and are high (1.3−1.6) hence suggested their high crystallisation temperature (Longhi, 1981).

Plagioclase analyses are presented in table 2 and their compositional range is shown in figure 5. Their composition evolved toward the decrease in Ca content from labrador ($Ab_{34.74–46.25}$ $An_{51.15–63.40}$) to albite type plagioclase ($Ab_{92.42–93.76}$ $An_{5.64–6.38}$) via andesine ($Ab_{55.14–64.54}$ $An_{35.12–44.96}$) and oligoclase ($Ab_{76.97–85.96}$ $An_{1.27–22.61}$). FeO contents are low (< 1 wt%) in Ca-plagioclases and relatively high (up to 2 wt%) in Na-types. F^{3+} is suspected in tetrahedral sites as Si does not reach the 3 cations (Si + Al < 3) in structural formulae.

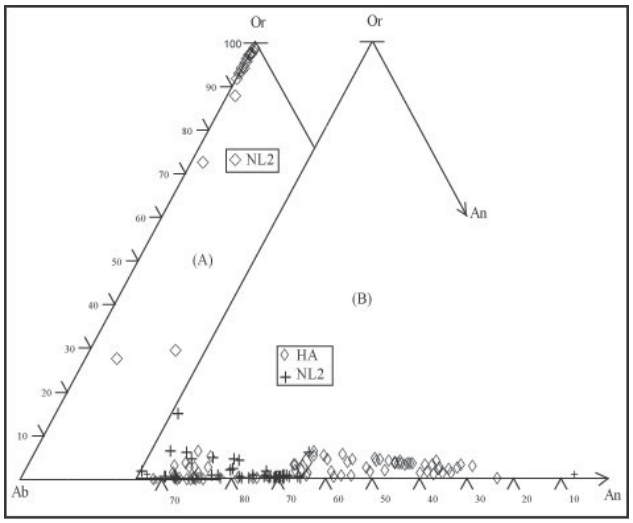

Figure 5. Feldspar composition of dolerite dyke swarm from Likok.

Table 2. Selected plagioclase analyses of doleritic dyke of Likok. Ph, c: phenocryst core ; ph, r: phenocryst rim

sample	NL0					NL1			NL2		NL3
description		Ph, r				Ph, c				Ph, r	
SiO_2 (wt %)	63.47	65.85	59.75	52.72	66.44	63.78	67.38	62.68	64.05	63.11	64.18
Al_2O_3	23.16	21.32	25.20	28.91	20.02	22.27	20.48	22.93	22.39	23.44	21.87
FeOt	0.47	0.60	0.19	0.60	0.46	0.06	0.15	0.17	0.50	0.07	0.88
CaO	4.62	2.33	7.58	13.12	1.38	3.60	1.21	4.52	3.81	4.77	3.13
Na_2O	9.09	10.36	7.70	3.97	11.06	9.94	11.15	9.10	9.49	8.96	9.49
K_2O	0.13	0.38	0.06	0.33	0.22	0.09	0.11	0.11	0.13	0.07	0.52
BaO	0.22	0.11	0.00	0.00	0.00	0.02	0.00	0.03	0.10	0.11	0.08
sum	101.16	100.95	100.49	99.65	99.58	99.77	100.49	99.54	100.46	100.53	100.14
Si (a.p.f.u.)	2.784	2.879	2.657	2.404	2.933	2.826	2.940	2.788	2.820	2.780	2.836
Al	1.197	1.099	1.320	1.554	1.042	1.163	1.053	1.202	1.162	1.217	1.139
Fe3+	0.017	0.022	0.007	0.023	0.017	0.002	0.005	0.006	0.018	0.003	0.033
Ca	0.217	0.109	0.361	0.641	0.065	0.171	0.057	0.215	0.180	0.225	0.148
Na	0.773	0.879	0.664	0.351	0.947	0.854	0.944	0.785	0.810	0.766	0.813
K	0.007	0.021	0.004	0.019	0.012	0.005	0.006	0.006	0.007	0.004	0.029
Ba	0.004	0.002	0.000	0.000	0.000	0.000	0.000	0.000	0.002	0.002	0.001
Or (%)	0.72	2.09	0.35	1.89	1.20	0.47	0.60	0.64	0.73	0.42	2.98
Ab	77.52	87.08	64.54	34.72	92.42	82.92	93.76	77.97	81.23	76.97	82.08
An	21.76	10.83	35.12	63.40	6.38	16.61	5.64	21.39	18.03	22.61	14.94

Table 3. Selected microprobe feldspar analyses of doleritic dyke of Likok. Ph, c: phenocryst core; ph, r: phenocryst rim

sample	NL0		NL1		NL2				NL3	
description	Ph, c			Ph, r				Ph, c		
SiO_2 (wt %)	63.12	63.30	63.26	63.22	63.59	66.05	66.85	63.88	63.59	63.93
Al_2O_3	18.69	18.59	18.95	21.61	18.79	20.10	19.96	19.03	18.66	18.85
FeOt	0.23	0.11	0.29	0.34	0.15	0.08	0.08	0.13	0.16	0.20
CaO	0.00	0.00	0.05	2.61	0.04	0.94	0.92	0.25	0.04	0.00
Na_2O	0.74	0.62	0.28	6.27	0.20	6.98	9.80	2.76	0.25	0.39
K_2O	15.31	15.34	15.57	6.07	16.01	5.56	2.27	11.91	15.87	15.89
BaO	1.36	1.80	2.38	0.28	1.87	0.95	0.78	1.64	1.65	1.37
sum	99.45	99.76	100.78	100.40	100.65	100.64	100.66	99.60	100.23	100.63
Si (a.p.f.u.)	2.953	2.964	2.949	2.823	2.959	2.954	2.941	2.960	2.967	2.962
Al	1.030	1.026	1.041	1.137	1.031	1.059	1.035	1.039	1.027	1.029
Fe	0.009	0.004	0.011	0.013	0.006	0.003	0.003	0.005	0.006	0.008
Ca	0.000	0.000	0.002	0.125	0.002	0.045	0.043	0.013	0.002	0.000
Na	0.067	0.056	0.025	0.543	0.018	0.606	0.836	0.248	0.023	0.035
K	0.914	0.917	0.926	0.346	0.950	0.317	0.128	0.704	0.945	0.939
Ba	0.025	0.033	0.043	0.005	0.034	0.017	0.013	0.030	0.030	0.025
Or (%)	93.19	94.23	97.13	34.10	97.97	32.76	12.66	72.97	97.43	96.40
Ab	6.81	5.77	2.62	53.59	1.83	62.59	83.02	25.73	2.34	3.60
An	0.00	0.00	0.26	12.31	0.20	4.65	4.32	1.30	0.23	0.00

Alkali feldspar (Table 3, Fig. 5) is dominantly orthoclase ($Or_{72.97–97.97}$ $Ab_{1.83–25.73}$) with small amount of albite ($Or_{12.66–34.10}$ $Ab_{53.59–83.02}$). FeO contents are low (< 0.4 wt%) and BaO contents are relatively high (up to 2.4 wt% BaO) and thus belong to the barium-bearing feldspar.

Oxides minerals are Ti-magnetite (6−10 wt% TiO_2 and 75−80 wt% FeO) and ilmenite (42−50 TiO_2 and 40−53 wt% FeO) in composition (Table 4).

Table 4. Representative oxides analyses of doleritic dyke of Likok. Ilm: Ilmenite. mt: Magnetite (abbreviation after Kretz. 1983)

sample	NL2			NL2
mineral	ilm		mt	
description	Ph. c			
SiO_2 (wt%)	5.24	0.06	0.06	0.07
TiO_2	44.23	50.47	11.44	10.20
Al_2O_3	0.59	0.00	0.07	0.07
Cr_2O_3	0.03	0.01	0.07	0.07
FeO	40.12	42.32	78.27	80.01
MnO	3.12	5.31	0.45	0.46
MgO	0.11	0.10	0.01	0.04
CaO	2.34	0.19		
sum	95.79	98.45	90.38	90.91
Si (a.p.f.u.)	0.269	0.003	0.003	0.003
Ti	1.705	1.946	0.345	0.305
Al	0.035	0.000	0.003	0.003
Cr	0.001	0.000	0.002	0.002
Fe+2	1.701	1.701	1.333	1.291
Mn	0.135	0.231	0.015	0.016
Mg	0.008	0.007	0.001	0.002
X'Usp			0.345	0.305

Table 5. Chemical analyses of apatite and titanite of dolerites dykes of Likok.

sample	NL2				NL1
mineral	apatite				titanite
SiO_2 (wt%)	3.16	3.87	17.19	0.98	30.77
TiO_2	0.05	0.04	0.17	0.00	28.91
Al_20_3	0.70	1.58	7.24	3.29	2.61
FeO	0.65	1.45	9.89	0.10	2.45
MnO	0.09	0.00	0.12	0.01	0.00
MgO	0.01	0.70	5.84	0.00	0.00
CaO	52.84	51.18	29.26	53.82	27.06
Na_2O	0.31	0.37	0.03	0.13	0.00
P_2O_5	43.36	41.23	27.61	44.37	0.00
Sum	101.17	100.41	97.35	102.68	92.53
Si (a.p.f.u.)	0.492	0.609	2.720	0.150	4.447
Ti	0.006	0.004	0.020	0.000	3.142
Al	0.128	0.292	1.349	0.594	0.222
Fe 2+	0.084	0.190	1.309	0.012	0.297
Mn	0.012	0.000	0.016	0.001	0.000
Mg	0.003	0.164	1.378	0.000	0.000
Ca	8.818	8.626	4.962	8.844	4.191
Na	0.093	0.112	0.010	0.039	0.000
P	5.717	5.491	3.699	5.761	0.000

They occur in all samples as euhedral or subhedral crystals enclosed by clinopyroxene or distribute around the biotite phenocrysts. Ilmenite crystals are Mn-rich (up to 5.1 wt% MnO) and Ti-magnetite crystals are TiO_2 depleted ($TiO_2 \leq 10$wt%) with X'Usp values between 0.19 and 0.35.

Calculation of equilibrium temperatures and f(O2) using the geothermobarometer of Anderson & Lindsley (1988) gives the temperature range of 670−680 °C and fO2 of 10^{-40}−10^{-23}. Needle shaped microphenocrysts and microlites of apatite (25−54 wt% CaO and 37−44 wt% P_2O_5, table 5) are frequently scattered in the groundmass. Rare titanite microphenocrysts (22−29 wt% TiO_2 and 26−27 wt% CaO, table 5) are also present in all dolerites samples. They are isolated or partially enclosed in feldspar and biotite phenocrysts.

Phenocrysts and microlites of biotite crystals occur in all samples. Their compositions are presented in table 6. They are rich in Al_2O_3 (13−17 wt%) and relatively low in TiO_2 contents (<1.5 wt%), in accordance with the enrichment of those elements in the tholeiitic basaltic liquid. All crystals are Fe-rich (Mg/Fe ratios between 0.86 and 1.36 and Fe/Fe+Mg > 0.50). The number of cations in Y-sites is below the theoretical value (6).

Table 6. Selected biotite microprobe analyses of doleritic dykes of Likok.

sample	NL2				
mineral	biotite				
SiO_2 (wt%)	36.26	37.64	37.95	37.97	38.66
TiO_2	0.26	0.66	0.22	0.69	0.44
Al_2O_3	14.20	14.35	14.74	14.57	14.34
FeO	18.08	18.01	18.54	18.94	17.73
MnO	0.18	0.17	0.18	0.14	0.14
MgO	13.69	12.35	13.48	11.95	12.85
CaO	0.26	0.02	0.09	0.10	0.01
Na2O	0.03	0.65	0.05	0.06	0.03
K_2O	9.28	9.44	9.60	9.58	10.06
BaO	0.16	0.00	0.00	0.00	0.00
Sum	92.39	93.30	94.84	93.99	94.26
Si (apfu)	5.699	5.834	5.786	5.850	5.911
Ti	0.031	0.077	0.025	0.080	0.051
Al	2.631	2.621	2.648	2.647	2.584
Al IV	2.301	2.166	2.214	2.150	2.089
Al VI	0.330	0.455	0.434	0.497	0.494
Fe	2.377	2.335	2.364	2.440	2.267
Mn	0.024	0.022	0.023	0.019	0.018
Mg	3.206	2.853	3.063	2.744	2.928
Ca	0.044	0.004	0.014	0.016	0.002
Na	0.009	0.196	0.015	0.017	0.009
K	1.860	1.867	1.867	1.883	1.962

4.4. Geochemistry

Major and trace element compositions of selected representative samples of Likok dolerites dyke swarms are presented in Table 7. Samples

exhibit the distinctly high and low contents of major and trace elements. They are hereafter distinguished as group I and group II according to their respective low (Mg: 53.0%) and high (Mg: 62.0−65.0%) Mg number (Mg: 100*[(MgO/40.32)/ (MgO/40.32) + (FeO/71.87))]. SiO_2 contents (48−52 wt%) of both groups are within the range of previously referenced continental tholeiites over the world (Carmichael et al., 1974): Karoo dolerites (50.6 to 53.6%), Tasmanian dolerites (53.8%), Antarctic Ferrar dolerites (53.0%), average eastern North American diabases (51.1%), Columbia River basalts (50.0 to 54.4%), Mayo Oulo-Léré and Babouri-Figuil dolerites (51.72%, Ngounouno et al., 2001), and Obudu dolerites of Nigeria in Benue Trough (44−52 wt%, Ekwueme, 1994) excepted those of doleritic dykes from Biden (58−59 wt%, Vicat et al., 2001).

Table 7. Representative whole-rock chemical analyses of dolerite dikes of Likok (NL1. NL2. NL3). IN29 is from Vicat et al., (2001). Les1 is from Ekwueme (1994) and NG105 is from Nkouandou et al., (2010).

sample	NL3	NL1	HA	NL2	IN29	Les1	NG105
SiO_2 (wt %)	51.26	48.17	48.14	51.49	58.88	50.23	41.66
TiO_2	2.33	1.37	2.88	2.22	1.55	1.68	4.50
Al_2O_3	12.76	14.12	13.91	12.87	14.94	15.37	14.59
Fe_2O_3	8.88	9.72	12.33	8.48	7.09	11.88	14.23
MnO	0.13	0.14	0.14	0.13	0.09	0.14	0.20
MgO	8.34	9.78	7.80	8.74	2.83	8.04	6.57
CaO	5.57	9.01	7.95	5.29	4.46	7.97	10.20
Na_2O	4.41	4.20	4.27	4.29	3.32	3.26	3.55
K_2O	4.96	2.93	2.10	5.21	4.23	0.48	0.92
P_2O_5	1.36	0.56	0.47	1.28	0.73	0.19	0.87
LOI	3.58	1.98	4.49	3.45	1.70	1.48	1.78
sum	100.00	100.00	100.00	100.00	99.82	100.72	99.07
CIPW norm							
Qtz	0.00	0.00		0.00	9.22	0.00	0.00
Ne	3.66	9.05	0.73	3.91	0.00	0	8.31
Hyp	0.00	0.00	0.00	0.00	12.64	0.00	0.00
Ol	11.40	10.20	9.67	12.41	0.00	7.07	13.95
Mg	62.6	64.2	53.0	64.8	47.3	65.90	63.7
D.I.	59.0	41.1	42.1	59.5	63.8	38.3	28.4
Rb (ppm)	133	85	66	143	160	6	45
Sr	1477	698	598	1450	736	289	967
Ba	2255	1339	430	2504	1715	17	564
Cr	158.51	195.20	31.69		60.40	253.00	25.50
Co	36.23	42.24	53.03		17.70	75.00	43.10
Ni	98.46	31.60	14.99		31.60	139.00	23.60
Cu	10.24	8.84	7.55			76.00	31.00
Zn	119.15	80.61	64.08			93.00	159.00
Y	24	31	28	23	19	23	32
Zr	412	195	207	385	336	86	435
Nb	23	9	17	21	24	11	87
Hf	4	4.6	6.5	4.4	8.1		9.3
Ta	1	0.6	0.7	0.9	1.6		5.9
Th	3.46	2.00	1.00	5.76	11.9		6.1
U	6.6	1.8	1.0	6.3		3	2
Pb	9.2	6.4	2.1		17.2	5.0	3.2

The relatively low contents of TiO_2 (mostly 1.4−2.9 wt%) classify those rocks into the low-Ti continental tholeiites as those described in West Africa (Marzoli et al., 2004) and Central Atlantic Magmatic Province (CAMP) of south-western Algeria (Moulley et al., 2010). Their Mg contents are relatively low (53.0-65.0%) and may not be consistent with those of primary liquids (Mg > 70, Roeder & Emslie, 1970) in equilibrium with the lherzolite mantle peridotites (containing high Fo olivine). The sums of Na_2O and K_2O are high (6.4 to 9.5 wt%) traducing their continental tholeiitic affinity (Campbell, 1985). Similar high alkali values characterised the intruded plutonic granite type of

Ngaoundéré (Tchameni et al., 2006) and Maiganga (Ganwa et al., 2008) of basement rocks. P_2O_5 contents are low (< 0.6 wt%) in group II dolerites and relatively high (1.4 wt%) in group I. P_2O_5/TiO_2 ratios are low (0.16-0.4) for primitive and high (0.6) for evolved dolerites.

Transitional elements, Ni (15−98 ppm), Co (36−53 ppm), Cr (32−195), Cu (8−10 ppm) and Zn (64−119 ppm) of all dolerites are low compared to primitive lavas directly produced through the melting of lherzolite mantle source with high Mg (90) and Ni (400−500 ppm) contents (Green et al., 1974). In Cr vs Y diagram (not shown) after Ohnenstetter et al., (1990), the studied dolerites display the parallel trend to clinopyroxene and plagioclase fractionation patterns.

Sr, Ba and Rb contents display a wide variation within each group. They are relatively low (Sr: 598−698 ppm, Rb: 66−85 ppm and Ba: 430−1339 ppm) in evolved group and high in primitive group (Sr: 1450−1477 ppm, Rb: 133−143 ppm and Ba: 2255−2504 ppm).

Incompatible element contents are low in group I and high in group II. Zr: 195−205 ppm and 385−412 ppm, Hf: 4.0−4.4 ppm and 4.6−6.5 ppm, Ta: 0.6 −0.7 ppm and 1−0.9 ppm, Nb: 9−17 ppm and 21−23 ppm, Th: 1−2 ppm and 3.5−7.8 ppm, U: 1.0−1.8 ppm and 6.3−6.6 ppm and Y: 28−31 ppm and 23−24 ppm. Ratios of high-field-strength elements (e.g. Zr/Hf and Nb/Ta) vary distinctly within each group. High values (103 and 23) are respectively found in group I while low values (32 and 15) are found in group II dolerites. There is a constant variation of mobile incompatible elements such as K, Rb, Sr, Ba or Th. K/Rb ratios are higher (260- 300) while Rb/Sr ratios are low (0.2) in all samples as have been indicated by Dupuy & Dostal (1984) in continental tholeiites. The group II dolerite samples exhibit the low Zr/Nb (12−21) and Zr/Y (6−7) ratios, while these ratios are high group I dolerites (Zr/Nb of 18 and Zr/Y of 17). The Nb/Y ratios (indicators of alkalinity) are low (0.29−0.58) in group I and relatively high (> 0.90) in group II. In the triangular Hf-Th-Nb (after Meschede, 1986), the Likok dolerites fall within the tholeiite magma affinity (Fig. 3).

Mantle-normalized trace elements of Figure 6 are quite parallel to the typical continental tholeiites studied worldwide (Holm, 1985; Vicat et al., 2001).

They are characterized by high contents of incompatible elements relative to the primitive mantle (up to 400 times). Normalized incompatible elements contents increase from K to Rb and decrease continuously to Y. All continental tholeiites patterns display the negative anomalies in Nb and Ta relative to the NG105 pattern which is typical alkali lava. Ba, P, Sr and Zr show the less pronounced positive anomalies on their patterns.

5. DISCUSSIONS

The field observations reveale the absolute vertical outcropping of the studied dykes. These observations might be related to the extension of the continental lithosphere at that time. Such crustal extension are attested by the geophysical data (Fairhead & Okereke, 1988; Poudjom Djomani et al., 1997) which suggest the lithosphere uplift by the upward migration of the lithosphere-asthenosphere boundary (Ambeh et al., 1989), enhanced by two broad negative gravity anomalies (–80 to –100 and –120 mGal/cm), consecutively to lithospheric (40 km) and crustal (20 km) thinning (Poudjom Djomani et al., 1997). The location in the E-MORB and WPT field of Likok dolerites also suggest that the dolerite dykes were formed during intra-plate extension. Those dykes strike mainly in the Pan-African fault directions (N70, N160 and N30) indicated by Moreau et al., (1987). Likok dykes swarm thus may be related to the Pan-African tectonic lineaments, which might have served as magma conduits during the cretaceous extension of Northern and Central Africa (Guiraud et al., 2005).

Mineral compositions reveal the complex petrogenetic evolutions which usually characterise the doleritic dykes of continental setting (Marsh, 1989; Seymour & Kumarapeli, 1995). The clinopyroxene compositions are shifting from Ca-rich (diopside) to Ca-poor (sub-calcic and pigeonite) with the increasing Fe^{2+} contents from the former to the later (Fig. 4). This might suggest that Ca-rich clinopyroxene crystallised before Ca-poor clinopyroxene as always suggested for tholeiitic lavas affinity (Longhi, 1981). Thus, the continuous decreasing Ca contents concomitantly with the increasing Fe^{2+} contents of clinopyroxene crystals is the strong argument of their parental magma differentiation by fractional crystallization, certainly during their crustal ascent. Fractional crystallization process is also attested by the progressive crystallisation of plagioclase from labradorite to albite and feldspar from orthoclase to albite.

Geochemical data suggest the existence of two different groups of dolerites dyke, derived probably from the same source by fractional crystallisation, thus suggesting the differentiation of the parental magma giving rise to the series of those dykes. Major elements of dolerites of group II exhibit the distinctly high SiO_2, Mg and alkali contents. The higher values of those elements probably indicate the low partial

melting at deeper depth. In this consideration, the group I dolerites probably represent the result of magma differentiation from group II dolerites by fractional crystallisation. Hence, the bimodal nature of those dolerites which excludes any crystal fractionation relation between the both groups (Sun et al., 2013) remains indicative. The very high alkali contents (Table 4) of lavas might results from a complex or second petrogenetic process as the indicators of alkalinity (Nb/Y) are low (< 1) compared to those of typical alkaline lavas (NG105, Nb/Y= 2.7) of the Adamawa plateau (Nkouandou et al., 2008) and Cameroon Volcanic Line (Kamgang et al., 2013). The low-Ti contents of Likok dykes have commonly been related to crustal contamination or the derivative of the lavas from the sub continental lithospheric mantle (Ewart et al., 1998 and 2004). The low contents of transitional elements (Ni, Cr and Co of the dolerites of both groups) attest the evolved character of their parental magma. In the spider diagram (Fig. 6), all samples show the moderate negative anomaly in Nb and the high contents of incompatible elements, indicating that they may originate from the mantle sources of sub continental composition (Arndt et al., 1993; Xu et al., 2001 and 2004). The geochemical variations within the two groups, not only accounted for by differentiation processes, could be explained by the contribution of a small amount of crustal contamination (due to negative Nb and Ta anomalies), which is currently hard to verify due to the absence of isotope data. Thus, crustal contamination is possibly not significant. A weak hydrothermal metasomatism (if present) may have happened during the ascending magma flows through the continental crust of group II dolerites as attested by the ratios of Z/Y (6-7, Brewer et al., 1992).

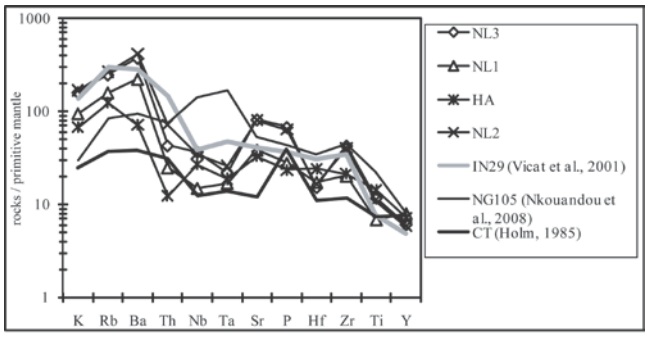

Figure 6. Likok continental dolerite trace elements normalized to Primitive Mantle (Sun & McDonough, 1989). Data of Miocene volcanism of Ngaoundéré (Nkouandou et al., 2008, sample NG105), doleritic dyke of Biden (Vicat et al., 2001) and Continental Tholeiite (Holm, 1985, mean of 32 samples) are added for comparison.

The orientation of Likok dykes are parallel to the main Pan-African directions established by Moreau et al., (1987). They also crosscut the Pan-African basement rocks, witnessing their late occurrence into the subsequence formations. Hence, the Likok dykes are possible fingerprints of the post-Pan-African extensional magmatism, related to the early stage of Pan-African break-up consecutively with the opening of the equatorial domain of the south Atlantic, initiated in Late Jurassic-Early Cretaceous time (Coulon et al., 1996; Guiraud et al., 2005). The same considerations have been suggested for the 140.5 ± 0.7 Ma Obudu dolerites dyke of the Benue Trough which has been interpreted as the product of basic magmatism related to the early stages of rifting along the Benue Trough of Nigeria (Ekwueme, 1994).

6. CONCLUSIONS

The dolerites dyke of Likok in Adamawa plateau display a chemical composition of intraplate continental quartz tholeiites, generated from a sub-continental mantle source sharing enriched asthenospheric E-MORB components. They are fingerprints of the post-Pan-African extensional magmatism, related to the early stage of Pan-African break-up consecutively with the opening of the equatorial domain of the south Atlantic, initiated in Late Jurassic-Early Cretaceous time.

ACKNOWLEDGMENTS

Authors thank the “Agence Universitaire de la Francophonie (AUF)” for financial support of this work through the project no. 51110SU201 and to Doctor Mitică Pintilei, PhD ("Alexandru Ioan Cuza" University of Iași, Romania) for the ED-XRF analysis.

REFERENCES

Ambeh, W.B., Fairhead, J.D., Francis, D.J., Nnange, J.M. & Djallo S., 1989. *Seismicity of the Mount Cameroon region West Africa*. J. Afr. Earth Sci., 5, 9, 1–7.

Andersen, D.J. & Lindsley, D.H., 1988. *Internally consistent solution models for Fe−Mg−Mn−Ti oxides; Fe−Ti oxides.* Am. Mineral., 73, 714−726.

Arndt, N.T., Czamanske, G.K., Wooden, J.L., Fedorenko, V.A., 1993. *Mantle and crustal contributions to continental flood volcanism.* Tectonophysics, 223, 39–52.

Béa, A., Cochemé, J.J., Trompette, R., Affaton, P., Soba, D., Sougy, J., 1990. *Grabens d’âge Paléozoïque inférieur et volcanisme tholéiitique associé dans la région de Garoua, Nord Cameroun*. Journal of African Earth Sciences, 10:

657–667.

Brewer, T.S., Hergt, J.M., Hawkesworth, C.J., Rex, D.& Storey, B.C., 1992. Coats *land dolerites and the generation of Antarctic continental flood basalts. In: Storey BC, Alabaster T, Pankhurst RJ (Eds.), Magmatism and the Causes of Continental Break Up*. Geol. Soc. Spec. Publ., 68, 185–208.

Bryan, S.E. & Ernst, R.E., 2008. *Revised definition of Large Igneous Provinces (LIPs).* Earth Sci. Rev., 86, 175–202.

Cabanis, B. & Thieblemont, D., 1988. *La discrimination des tholéiites continentales et des basaltes arrière-arc. Proposition d'un nouveau diagramme Th–Tbx3–Tax2.* Bulletin de la Société Géologique de France, 8,6, 927−935.

Campbell, I.H., 1985. *The difference between oceanic and continental tholeiites : a fluid dynamic explanation.* Contrib. Mineral. Petrol., 91, 37−43.

Carmichael, I.S.E., Turner, F.J. & Verhoogen, J., 1974. *Igneous Petrology*. McGraw−Hill, New York.

Coulon, C., Vidal, P., Dupuy, C., Baudin, P., Popoff, M., Maluski, H. & Hermitte, D., 1996. *The Mezozoic to eraly Cenozoic magmatism of the Benue trough (Nigeria), geochemical evidence for the involvement of the St Helene plume.* J. Petrol., 37, 1341−1358.

Déruelle, B., NGounouno, I., Demaiffe, B., 2007. *The Cameroon Hot Line (CHL): a unique example of active alkaline intraplate structure in both oceanic and continental lithospheres.* C R Geosci., 339, 589–600.

Dupuy, C. & Dostal, J., 1984. *Trace element geochemistry of some continental tholeiites.* Earth Planet. Sci. Lett., 67, 61−69.

Ekwueme, B.N., 1994. *Basaltic magmatism related to the early stages of rifting along the Benue Trough: the Obudu dolerites of south-east Nigeria.* Geol. J., 29, 269−276.

Essany, M.A. & EL−Metwally, A.A., 1999. *Petrogenesis of a high TiO_2 mafic dyke swarm from southwest Sinai.* J. Afr Earth Sci., 29, 3, 551−565.

Ewart, A., Marsh, J.S., Milner, S.C., Duncan, A.R., Kamber, B.S. & Armstrong, R.A., 2004. *Petrology and geochemistry of Early Cretaceous bimodal continental flood volcanism of the NW Etendeka, Namibia, part 1: introduction, mafic lavas and reevaluation of mantle source components.* J. Petrol., 45, 59–105.

Ewart, A., Milner, S.C., Armstrong, R.A. & Duncan, A.R., 1998. *Etendeka volcanism of the Goboboseb Mountains and Messum Igneous Complex, Namibia. Part I: geochemical evidence of Early Cretaceous Tristan plume melts and the role of crustal contamination in the Paraná–Etendeka CFB.* J. Petrol., 39, 191–225.

Fairhead, J.D. & Okereke, C.S., 1988. *Depths to major density contrasts beneath the West African rift system in Nigeria and Cameroon based on the spectral analysis of gravity data.* J. Afr. Earth Sci., 7, 769–777.

Floyd, P.A. & Winchester, J.A., 1975. *Magma type and tectonic setting discrimination using immobile elements.* Earth planet. Sci. Lett., 27, 211−218.

Ganwa, A.A., Frisch, W., Siebel, W., Ekodeck, G.E., Cosmas, S.K. & Ngako, V., 2008. *Archean inheritances in the pyroxene-amphibole bearing gneiss of the Méiganga area (Central North Cameroon): Geochemical and 207Pb/206Pb age imprints.* C. R. Géoscience, 340, 211–222.

Green, T.H., Edgar, A.D., Beasley, P., Kiss, E. & Ware, N.G., 1974. *Upper mantle source for some hawaiites, mugearites and benmoreites.* Contrib. Mineral., 48, 33–43.

Guiraud, R., Bosworth, W., Thierry, J., Delplanque, A., 2005. *Phanerozoic geological evolution of Northern and Central Africa: An overview.* J. Afr. Earth Sci., 43, 83–143.

Holm, P.E., 1985. *The geochemical fingerprints of different tectonomagmatic environment using hygromagmatophile element abundance of tholeiitic basalts and basaltic andesites.* Chem. Geol., 51, 303−323.

Kamgang, P., Chazot, G., Njonfang, E., Blaise, N., Ngongang, T. & Tchoua, F.M., 2013. *Mantle sources and magma evolution beneath the Cameroon Volcanic Line: Geochemistry of mafic rocks from the Bamenda Mountains (NW Cameroon).* Gond. Res., 24, 2, 727−741.

Kampunzu, A.B. & Popoff, M., 1991. *Distribution of the main Phanerozoic African rifts and associated magmatism: introductory notes. In: Kampunzu AB, Lubala RT (eds). Magmatism in Extensional Structural Settings, the Phanerozoic African Plate.* Springer-Verlag: Berlin, 2–10.

Kretz, R., 1983. *Symbols for rock-forming minerals***.** Am. Mineral., 68: 277–279.

Le Bas, M.J., Le Maitre, R.W., Streckeisen, A.L. & Zanettin, P., 1986. *A chemical classification of volcanic rocks based on the total alkali-silica diagram.* J. Petrol., 27, 745–750.

Longhi, J., 1981. *Multicomponent phase diagrams and the phase equilibria of basalts. In Workshop on Magmatic Processes of Early Planetary Crusts.* LPI Technical Report, 82, 1, 90−94.

Marsh, J.S., 1989. *Geochemical constraints on coupled assimilation and fractional crystallization involving upper crustal compositions and continental tholeiitic magma.* Earth Planet. Sci. Lett., 92, 70−80.

Marzoli, A., Bertrand, H., Knight, K., Cirilli, S., Buratti, N., Verati, C., Nomade, S., Renne, P.R., Youbi, N., Martini, R., Allenbach, K., Neuwerth, R., Rapaille, C., Zaninetti, L. & Bellieni, G., 2004. *Synchrony of the Central Atlantic Magmatic province and the Triassic–Jurassic boundary climatic and biotic crisis.* Geol., 32: 973–976.

Marzoli, A., Chiaradia, M., Jourdan, F., Bussy, F.,

2006. *Parental magmas and crustal contamination of continental tholeiitic basalts from the Central Atlantic magmatic province as revealed by mineral major and trace elements and Sr isotopes.* Goldschmidt Conference Abstracts., doi:10.1016/j.gca.06.801

Meschede, M., 1986. *A method of discriminating between different types of mid-ocean ridge basalts and continental tholeiites with the Nb-Zr-Y diagram.* Chem. Geol., 56, 207−218.

Moreau, C., Regnoult, J.-M., Déruelle, B., Robineau, B., 1987. *A new tectonic model for the Cameroon Line, central Africa.* Tectonophysics, 139, 317–334.

Morimoto, N., Fabriès, J., Ferguson, A.K., Ginzburg, I.V., Ross, M., Seifert, F.A., Zussman, J., Aoki, K. & Gottardi G., 1988. *Nomenclature of pyroxenes*. Mineral. Mag., 52: 535–550.

Moulley, C.C., Bertrand, H., Sebaï, A., 2010. *Geochemistry of the Central Atlantic Magmatic Province (CAMP) in south-western Algeria*. J. Afr. Earth Sci., 58, 211–219.

Ngounouno, I., Déruelle, B., Guiraud, R., Vicat, J.-P., 2001. *Magmatismes tholéiitique et alcalin des demi-grabens crétacés de Mayo Oulo–Léré et de Babouri–Figuil (Nord du Cameroun–Sud du Tchad) en domaine d'extension continentale.* C. R. Acad. Sci., 333, 201-207.

Nkouandou, O.F., Ngounouno, I., Déruelle, B., Ohnenstetter, D., Montigny, R. & Demaiffe, D., 2008. *Petrology of the Mio–Pliocene volcanism to the North and East of Ngaoundéré (Adamawa, Cameroon).* C. R. Geosci., 340, 28–37.

Nkouandou, O.F., Ngounouno, I., Déruelle, B., 2010. *Géochimie des laves basaltiques récentes des zones Nord et Est de Ngaoundéré (Plateau de l'Adamaoua, Cameroun, Afrique Centrale): pétrogenèse et nature de la source.* Int. J. Biol. Chem. Sci., 4, 4, 984–1003.

Ohnenstetter, M., Bechon, F., Ohnenstetter, D., 1990. *Geochemistry and mineralogy of lavas from the Arakapas Fault Belt, Cyprus — consequences for Magma Chamber Evolution.* Mineral. Petrol., 41, 105–124.

Pearce, J.A. & Cann, J.R., 1973. *Tectonic setting of basic volcanic rocks determined using trace element analysis.* Earth Planet. Sci. Lett., 19, 290-300.

Popoff, M., 1988. *Du Gondwana à l'Atlantique Sud: les connections du fossé de la Bénoué avec les basins du Nord-Est Brésilien jusqu'à l'ouverture du Golfe de guinée au Crétacé inférieur.* Journal of African Earth Sciences, 7, 2, 409-431.

Pouchou, J.L. & Pichoir, F., 1991. *Quantitative analysis of homogeneous or stratified microvolumes applying the model "PAP". In: Heinriche, D. E. (ed) Electron Probe Quantification.* Plenum Press, New York, 31–75.

Poudjom Djomani, Y.H., Diament, M. & Wilson, M., 1997. *Lithospheric structures across the Adamawa Plateau (Cameroon) from gravity studies.* Tectonophysics, 273, 317–327.

Reeves, C., 2000. *The geophysical mapping of Mesozoic dyke swarms in southern Africa and their origin in the disruption of Gondwana.* J. Afr. Earth Sci., 30,3, 499−513.

Roeder, P.L. & Emslie RF., 1970. *Olivine-liquid equilibrium.* Contrib. Mineral. Petrolo., 29, 275−289.

Seymour, K.S. & Kumarapeli, P.S., 1995. *Geochemistry of the Grenville Dyke Swarm: role of plume−source mantle in magma genesis.* Contrib. Mineral. Petrol., 120, 29−41.

Srivastava, R.K., 2011. *Dyke Swarms: Keys for Geodynamic Interpretation.* Springer-Verlag: Berlin.

Sun, M.D., Chen, H.L., Zhang, F.Q., Wilde, S.A., Dong, C.W. & Yang, S.F., 2013. *A 100 Ma bimodal composite dyke complex in the Jiamusi Block, NE China: An indication for lithospheric extension driven by Paleo-Pacific roll-back.* Lithos, 162-163, 317–330.

Sun, SS. & McDonough, W.F., 1989. *Chemical and isotopic systematics of oceanic basalts: implications for the mantle composition and processes. In: Saunders AD and Norry MJI (Eds.), Magmatism in the Ocean Basins.* Geol. Soc. London Publ., 42, 313−345.

Tchameni, R., Pouclet, A., Penaye, J., Ganwa, A.A., Toteu, S.F., 2006. *Petrography and geochemistry of the Ngaoundéré Pan-African granitoids in central north Cameroon: implications for their sources and geological setting.* J. Afr. Earth Sci., 44, 511–529.

Vicat, J.−P., Ngounouno, I. & Pouclet, A., 2001. *Existence des dykes de dolérites anciens à composition de tholéiite continental dans la province alcaline de la Ligne du Cameroun. Implication du contexte géodynamique.* C. R. Geosci., 332, 243–249.

Vicat, J.−P., Polklet, A., Nkoumbou, C. & Mouangue, A.S., 1997. *Le volcanisme fissural néoprotérozoique des séries du Dja inférieur, de Yokadouma (Cameroun) et de Nola (RCA) - Signification géotectonique.* C. R. Geosci., 326, 671−677.

Worthing, M.A., 2005. *Petrology and geochronology of a Neoproterozoic dyke swarm from Marbat, South Oman.* Journal of African Earth Sciences, 41, 248–265.

Xu, Y., Chung, S.L., Jahn, B.-M. & Wu, G., 2001. *Petrologic and geochemical constraints on the petrogenesis of Permian–Triassic Emeishan flood basalts in southwestern China*. Lithos, 58, 145–168.

Xu, Y., He, B., Chung, S.L., Menzies, M.A. & Frey, F.A., 2004. *Geologic, geochemical, and geophysical consequences of plume involvement in the Emeishan flood-basalt province.* Geol., 32, 917–920.

Received at: 03. 02. 2014
Revised at: 29. 10. 2014
Accepted for publication at: 28. 12. 2014
Published online at: 13. 01. 2015